University of Groningen

SK channel activation potentiates auranofin-induced cell death in glio- and neuroblastoma cells

Krabbendam, Inge E; Honrath, Birgit; Bothof, Laura; Silva-Pavez, Eduardo; Huerta, Hernán; Peñaranda Fajardo, Natalia M; Dekker, Frank; Schmidt, Martina; Culmsee, Carsten; César Cárdenas, Julio

IMPORTANT NOTE: You are advised to consult the publisher's version (publisher's PDF) if you wish to cite from it. Please check the document version below.

Document Version
Publisher's PDF, also known as Version of record

Link to publication in University of Groningen/UMCG research database

SK channel activation potentiates auranofin-induced cell death in glio- and neuroblastoma cells

Inge E. Krabbendam[a,*], Birgit Honrath[a], Laura Bothof[a], Eduardo Silva-Pavez[b], Hernán Huerta[b], Natalia M. Peñaranda Fajardo[c], Frank Dekker[d], Martina Schmidt[a], Carsten Culmsee[e,f], Julio César Cárdenas[b,g,h], Frank Kruyt[c], Amalia M. Dolga[a,*]

[a] Faculty of Science and Engineering, Department of Molecular Pharmacology, Groningen Research Institute of Pharmacy (GRIP), University of Groningen, 9713 AV Groningen, the Netherlands
[b] Center for Integrative Biology, Faculty of Sciences, Universidad Mayor, Chile and Geroscience Center for Brain Health and Metabolism, Santiago, Chile
[c] Department of Medical Oncology, University of Groningen, University Medical Center Groningen, Groningen, the Netherlands
[d] Department of Chemical and Pharmaceutical Biology, Groningen Research Institute of Pharmacy (GRIP), University of Groningen, Groningen, the Netherlands
[e] Institut für Pharmakologie und Klinische Pharmazie, Biochemisch-Pharmakologisches Centrum Marburg, Philipps-Universität Marburg, Karl-von-Frisch-Straße 2, Marburg 35032, Germany
[f] Center for Mind, Brain and Behavior, Universities of Marburg and Gießen, Hans-Meerwein-Straße 6, 35032 Marburg, Germany
[g] Buck Institute for Research on Aging, Novato, CA 94945, United States
[h] Department of Chemistry and Biochemistry, University of California, Santa Barbara, CA 93106, United States

A B S T R A C T

Brain tumours are among the deadliest tumours being highly resistant to currently available therapies. The proliferative behaviour of gliomas is strongly influenced by ion channel activity. Small-conductance calcium-activated potassium (SK/K_{Ca}) channels are a family of ion channels that are associated with cell proliferation and cell survival. A combined treatment of classical anti-cancer agents and pharmacological SK channel modulators has not been addressed yet. We used the gold-derivative auranofin to induce cancer cell death by targeting thioredoxin reductases in combination with CyPPA to activate SK channels in neuro- and glioblastoma cells. Combined treatment with auranofin and CyPPA induced massive mitochondrial damage and potentiated auranofin-induced toxicity in neuroblastoma cells *in vitro*. In particular, mitochondrial integrity, respiration and associated energy generation were impaired. These findings were recapitulated in patient-derived glioblastoma neurospheres yet not observed in non-cancerous HT22 cells. Taken together, integrating auranofin and SK channel openers to affect mitochondrial health was identified as a promising strategy to increase the effectiveness of anti-cancer agents and potentially overcome resistance.

1. Introduction

Brain tumours, such as neuroblastomas in children and gliomas in adults, are the most frequent and deadly primary brain tumours. Neuroblastoma is a developmental tumour in children derived from the embryonic neural crest. Currently, neuroblastoma is the primary cause of death from paediatric cancer for children below the age of 5 years [1,2]. Gliomas are primary brain tumours that arise from glial cells. Based on their histopathological and genetic features, they are classified into different pathological grades with grade IV or glioblastoma multiforme (GBM) being the most severe, proliferative, invasive and resistant to current therapeutic strategies [3–5]. Major hallmarks of cancer include impaired regulation of cell invasion, proliferation, apoptosis or cell cycle control, which have also been linked to the activity of ion channels [6–9]. Among ion channels, the identification and characterization of calcium-activated potassium (K_{Ca}) channels in tumour cells has gained interest in the cancer field. Indeed, K_{Ca} channel subtypes have been found in grade IV glioma cells [10] and opening of the large-conductance K_{Ca} (BK) channel has been shown to induce cell death in glioma cells [11,12]. Small-conductance K_{Ca} (SK) channels, that belong to the same family as the BK and intermediate-conductance K_{Ca} (IK) channels, are associated with cell cycle progression, migration/invasion, cell volume control and apoptosis [13,14]. SK channels are expressed in several cancer cell types, such as human melanoma cells and breast cancer cells, and have been implicated in processes related to cancer cell survival [15,16].

In healthy brain cells, pharmacological SK channel activation with CyPPA, led to a mild decrease in mitochondrial respiration and a moderate increase in mitochondrial reactive oxygen species (ROS) [14]. The higher aerobic glycolytic activity of cancer cells drives their

intracellular ROS production, resulting in a shift in redox balance, which promotes mutations and metabolic adaptations that facilitate extremely rapid tumour growth and cancer progression. When ROS accumulation reaches such a high level, the cell is being exposed to severe oxidative stress [17–20]. However, many cancer cells are equipped with strong antioxidant defence mechanisms in order to adapt to elevated ROS and to avoid apoptosis [21,22]. Despite the elevated antioxidant defence mechanisms and high ROS levels in cancer cells, it has been reported that these cells are vulnerable to further increases in ROS levels [23,24]. Therefore, we hypothesize that SK channel activation might accelerate cell toxicity mediated by current therapies aimed at increasing ROS levels. Indeed, current cancer treatments aimed to further enhance intracellular and mitochondrial ROS production have been proven as efficient approaches to induce the demise of cancer cells. For example, compounds that target mitochondria trigger overproduction of ROS, induce mitochondrial permeability transition pore (mPTP) formation, depolarise mitochondrial transmembrane potential, and lead to cell death [25,26]. One type of ROS-inducing compounds is the gold-derivative auranofin which can inhibit both cytosolic and mitochondrial thioredoxin reductase (TrxR) [27]. The thioredoxin system, composed of thioredoxin (Trx), TrxR, and NADPH, plays a critical role in regulating cellular redox homeostasis [27,28]. In many tumour cells, TrxR is overexpressed which has been implicated in the resistance of several human tumour cells against chemotherapeutics [27,29,30]. Auranofin-induced cell death is mediated by inhibiting the activity of both TrxR and glutathione peroxidase (GPx) [31] that lead to high ROS levels in the cytosol and mitochondria, cytochrome *c* release, increased mitochondrial Bax, and ultimately to cell death [32–34]. Auranofin was recently evaluated in clinical studies for treating chronic lymphocytic leukemia, lung cancer and ovarian cancer (see www.clinicaltrials.gov trial numbers NCT01419691, NCT01737502, NCT01747798, and NCT03456700).

To our knowledge, the combination treatment of auranofin and SK channel modulation has not been reported for antitumour activity. The similarity in terms of inducing cellular damage via ROS accumulation prompted us to investigate the effect of combined treatment of auranofin and CyPPA in brain cancer cells. Treatment based on reducing cancer cells' antioxidant defense with auranofin and SK channel activation was studied in neuroblastoma and glioblastoma cell lines as well as in patient-derived GBM neurospheres. In addition, we studied whether adding a ROS inducer might damage non-cancerous HT22 cells. We evaluated the effects of auranofin and CyPPA combination treatment on mitochondrial integrity and cell death. We show that auranofin induces cell death in a concentration-dependent manner, by affecting mitochondrial integrity and respiration. SK channel activation potentiated auranofin-induced toxicity, indicating that this combination treatment may have efficacy in brain tumours.

2. Materials and methods

2.1. Cell culture

A neuroblastoma cell line (SK-N-AS), a glioblastoma U251 cell line and a non-cancerous, immortalized neuronal cell line (HT22) were studied. Cells were cultured in Dulbecco's modified Eagle Medium (DMEM high glucose; Gibco, Fisher Scientific, Landsmeer, the Netherlands), supplemented with 10% fetal bovine serum (FBS; GE Healthcare Life Sciences, Eindhoven, the Netherlands), 100U/mL penicillin, and 100 µg/mL streptomycin, thereafter termed complete DMEM, at 37 °C and 5% CO_2. Complete DMEM was supplemented with 1% non-essential amino acids for SK-N-AS, 1% sodium pyruvate for HT22 and Antibiotic-Antimycotic (1X) (Gibco Life Technologies, USA) for U251 cells. HT22 and SK-N-AS cells were harvested using Trypsin/EDTA, and neurospheres were dissociated by accutase (Sigma-Aldrich, Zwijndrecht, the Netherlands). Penicillin, streptomycin, non-essential amino acids, sodium pyruvate and Trypsin/EDTA are bought from

Fisher Scientific. The passage number used in this study ranged between 300 and 350 for HT22 cells, 20–30 for U251 and 10–20 for SK-N-AS and GBM neurospheres. HT22 cells were kindly provided by Prof. Carsten Culmsee (University of Marburg, Germany). SK-N-AS cells were obtained from ATCC (Manassas, VA, USA). U251 cells were kindly provided by Dr Claudio Hetz (University of Chile).

For the generation of U251 spheroids, a 96-well plate was treated with 1% w/v low melting point agarose (Cleaver Scientific, UK) solution in MEM (Gibco Life Technologies, USA) without FBS to generate a low adhesion surface. After solidification of the agarose, 10.000 cells plus 10 µg/mL collagen I (Gibco Life Technologies, USA) were added per well. The plate was then centrifuged at 1000 rpm for 10 min and maintained under standard cell culture conditions. After 5–7 days when spheroids looked compact, showed a regular shape and defined borders, they were transferred to a 12-well invasion plate. The invasion plate was pre-treated with 1.25 mL of 2.2 mg/mL collagen I for 5 min, followed by washing and embedding a collagen I gel matrix made of 2 mL of 3 mg/mL collagen I supplemented with 250 µL of MEM-10X (Gibco Life Technologies, USA) and 600 µL 0.1 M NaOH (Merck Millipore, USA). The whole procedure was performed at ice-cold temperature, including the materials. The media containing the treatment was changed every 48 h.

The GBM neurospheres GG16 were generated from surgical leftovers obtained from anonymous GBM patients, as described before [35], after approval and following the ethical guidelines of the Medical Ethics Review Committee (METC) of the University Medical Center Groningen (UMCG). Cells were propagated as neurospheres in neural stem cell medium, composed of Neurobasal A Medium (Gibco Life Technologies, Bleiswijk, The Netherlands) supplemented with 2% B27 supplement (Gibco Life Technologies), 20 ng/mL EGF (R&D systems, Abingdon, UK), 20 ng/mL bFGF (Merck-Millipore, Billerica, MA, USA), 1% penicillin, 1% streptomycin and 1% L-glutamine (Gibco Life Technologies). Cells were maintained at 37 °C and 5% CO_2.

When indicated, cells were treated with 1-Thio-β-D-glucopyranose atotriethylphosphine gold-2,3,4,6-tetraacetate (Auranofin; Tocris Bioscience, Bristol, UK) with concentrations ranging from 0.5 µM to 10 µM and with SK2/SK3 channel activator Cyclohexyl-[2-(3,5-dimethyl-pyrazol-1-yl)-6-methyl-pyrimidin-4-yl]-amine (CyPPA; generated by the group of Prof. Dr. F. J. Dekker, University of Groningen) at a concentration of 10–50 µM. All cell lines were regularly tested for Mycoplasma contamination and the study was performed with Mycoplasma free cells.

2.2. Cell viability assay

In HT22, SK-N-AS and U251 cells, cell viability was determined based on metabolic activity using the 3-(4,5-dimethylthiazol-2-yl)-2,5-diphenyltetrazolium bromide assay (MTT; Sigma-Aldrich, Zwijndrecht, the Netherlands) as described [36]. The absorbance was measured with the Synergy H1 Multi-Mode reader (Biotek, Winooski, Vermont, USA) at 570 nm and 630 nm as a reference. Values of non-treated control cells were normalized to 100% with which values of the treated cells were compared. Data were collected from six wells per condition.

In GBM GG16 cells, cell viability was determined based on the 3-(4,5-dimethylthiazol-2-yl)-5-(3-carbox-ymethoxyphenyl)-2-(4-sulfo-phenyl)-2H-tetrazolium assay (MTS; Promega, Leiden, the Netherlands). After addition of 20 µL/well of the CellTiter 96® AQueous One Solution Reagent and incubation of 4 h at 37 °C and 5% CO_2, absorbance was measured at 490 nm. The background absorbance of cell-free wells was subtracted from every measurement and values of non-treated control cells were normalized to 100% with which values of the treated cells were compared. Data were collected from six wells per condition.

2.3. Cell death assay by AnnexinV/PI or PI

To study cell death, AnnexinV/PI (Fisher Scientific, Landsmeer, the Netherlands) double staining was performed as described [37]. Flow cytometric analysis was performed using the Cytoflex (Beckman Coulter, Woerden, the Netherlands). AnnexinV$^-$, propidium iodide (PI)- and AnnexinV$^+$PI positive cells were counted as dead cells. Data were collected from 15 000 cells in triplicate per condition. Cell death of U251 cells was evaluated using the ability of cells to exclude PI (Fisher Scientific, USA). The level of PI incorporation was quantified in a FACScan flow cytometer (Becton-Dickinson, San Jose, CA). PI-positive subpopulations of U251 cells were considered dead. Experiments were repeated at least three times with cells of independent cell passage numbers.

2.4. Proliferation assay by crystal violet

Complementing PI measurement in U251 cells, a crystal violet assay was performed. Following treatment, U251 cells were washed with PBS-1X and stained with 0.5% crystal violet (Sigma-Aldrich, USA) in 20% methanol for 1 h. Then 200 μL methanol was added to each well and the absorbance was measured at 570 nm.

2.5. Measurement of mitochondrial parameters

Mitochondrial health was assessed through the use of different stainings and subsequent flow cytometric analysis as described [2,4] using the CytoFLEX (Beckman Coulter, Woerden, the Netherlands). Rhodamine-2-acetoxymethylester dye (Rho2-AM, Abcam, Cambridge, UK) was used for mitochondrial calcium, MitoSOX dye (Fisher Scientific, Landsmeer, the Netherlands) for mitochondrial superoxides and tetramethylrhodamine-ethyl ester (TMRE; Fisher Scientific, Landsmeer, the Netherlands) for the mitochondrial membrane potential ($\Delta\psi_m$). Data were recorded from 15,000 cells in triplicate per condition. Experiments were repeated at least three times with cells of independent cell passage numbers.

2.6. Seahorse XF analysis

To study effects on cell metabolism, Seahorse Extracellular Flux Analysis was used. HT22 and SK-N-AS cells were seeded in Seahorse XF 96-well plates (Seahorse Biosystems, Agilent Technologies, Waldbronn, Germany). Following treatment, the medium was removed and replaced by 180 μL assay medium containing 2 mM L-glutamine (Fisher Scientific, Landsmeer, the Netherlands), 1 mM pyruvate and 25 mM glucose (pH 7.35) and the plate was incubated for 1 h at 37 °C without CO$_2$. The Seahorse XF Biosystem was used to analyse oxygen consumption rate (OCR) and extracellular acidification rate (ECAR). Three baseline measurements (3 × min mix, 0 min delay, 3 min measure = 3/0/3) were recorded, followed by by injection of 4 μM oligomycin (3/0/3), 50 μM dinitrophenol (DNP) (3/0/3), 150 nM rotenone and 1 μM Antimycin A, and 50 mM 2-deoxy-D-glucose (2-DG) (3/0/3) for HT22 cells and 2 μM oligomycin (3/0/3), 1 μM carbonyl cyanide-4-(trifluoromethoxy) phenylhydrazone (FCCP) (3/0/3), 500 nM rotenone and 1 μM Antimycin A, and 50 mM 2-deoxy-D-glucose (2-DG) (3/0/3) for SK-N-AS cells. Substances oligomycin, DNP, rotenone, Antimycin A, 2-DG, pyruvate and glucose were bought from Sigma-Aldrich (Zwijndrecht, the Netherlands) After injection of each compound, OCR and ECAR were determined. Data were collected from six wells per condition and normalized to protein content to correct for treatment effects.

2.7. Measurement of soluble and lipid ROS

Soluble ROS were detected by H$_2$DCFDA dye (Fisher Scientific, Landsmeer, the Netherlands) and lipid peroxides were analysed by BODIPY dye (Fisher Scientific, Landsmeer, the Netherlands) as described [2,4] using the CytoFLEX (Beckman Coulter, Woerden, the Netherlands). Data were recorded from 15,000 cells in triplicate per condition. Experiments were repeated at least three times with cells of independent cell passage numbers.

2.8. Statistics

Statistical significance was assessed using one-way analysis of variance (ANOVA) followed by Tukey's comparison (GraphPad Prism 5.0) unless otherwise stated. FACS experiments were repeated at least three times with cells of independent cell passage numbers and contained at least three technical replicates. MTT and Seahorse XF experiments were also repeated at least three times with cells of independent cell passage numbers, containing six technical replicates.

3. Results

3.1. SK channel activation potentiates auranofin-induced cell death in SK-N-AS cells

First, analysed the effects of single auranofin (0.5–10 μM) treatment on cell viability in neuroblastoma cell line SK-N-AS. As a control, the neuronal hippocampal HT22 cell line was used. Auranofin reduced cell viability in a dose-dependent manner during both 6 and 24 h in both SK-N-AS and HT22 cells (Fig. 1B–E), as shown in an MTT assay. Interestingly, only 24 h was enough in SK-N-AS cells to lower 50% of cell viability with 2 μM auranofin, while in HT22 this damage was achieved in 6 h. However, MTT assay is primarily a measure for the metabolic activity of the cells, only indirectly allowing for estimating cell viability. Therefore, we also investigated cell morphology after 6 h of auranofin exposure, and observed cell rounding and detachment, morphological cell changes that suggested cytotoxicity, in both SK-N-AS cells (Fig. 1A, upper panels) and HT22 cells (Fig. 1A, lower panels). In addition, we checked cell death at 24 h following auranofin exposure by AnnexinV/PI stainings and FACS analysis. SK-N-AS cells showed more cell death compared to HT22 cells (Fig. 2B and C).

Next, we studied the combined effects of auranofin and SK channel activation by CyPPA (10–50 μM) on cell viability in SK-N-AS and HT22 cells after 6 and 24 h by FACS analysis of AnnexinV/PI (Fig. 2A–C). As shown before, auranofin significantly reduced cell viability compared to controls. In contrast to our expectations based on cell morphology and MTT assay, auranofin and the co-treatment with CyPPA did not affect cell death in HT22 cells after 6 h (Fig. 2A). Prolonging auranofin exposure to 24 h induced cell death, but there was no additional effect on cell death by adding CyPPA treatment (Fig. 2B). In contrast, in SK-N-AS cells, combined auranofin and CyPPA treatment led to a dose-dependent increase in cell death (Fig. 2C). Annexin/PI analysis showed that CyPPA alone had no impact on cell viability in HT22 cells in a concentration range of 10–50 μM, while in SK-N-AS cells it reduced cell viability at 50 μM which might explain the observation that CyPPA potentiated the auranofin-induced cell death in neuroblastoma SK-N-AS cells. These results suggest that SK channel activation potentiates auranofin-induced toxicity in neuroblastoma SK-N-AS cells.

To test whether SK channel activation increased the auranofin toxicity also in a human glioblastoma cell line, we applied the combined treatment strategy in U251 cells. Auranofin (2 μM) treatment did not affect the cellular viability of U251 cells after 24 h (see Fig. 2D) as measured by MTT assay. Only the combined treatment of auranofin and 50 μM CyPPA showed a strong reduction without reaching statistical significance. As shown in Fig. 2E, U251 cells treated for 24 h with auranofin showed significantly decreased cell viability, as measured by crystal violet assay. On the other hand, CyPPA alone was not affecting cell proliferation at any concentration. Finally, combined treatment of auranofin and CyPPA further decreased U251 cell viability. As shown in Fig. 2F, neither auranofin nor CyPPA were able to induce cell death
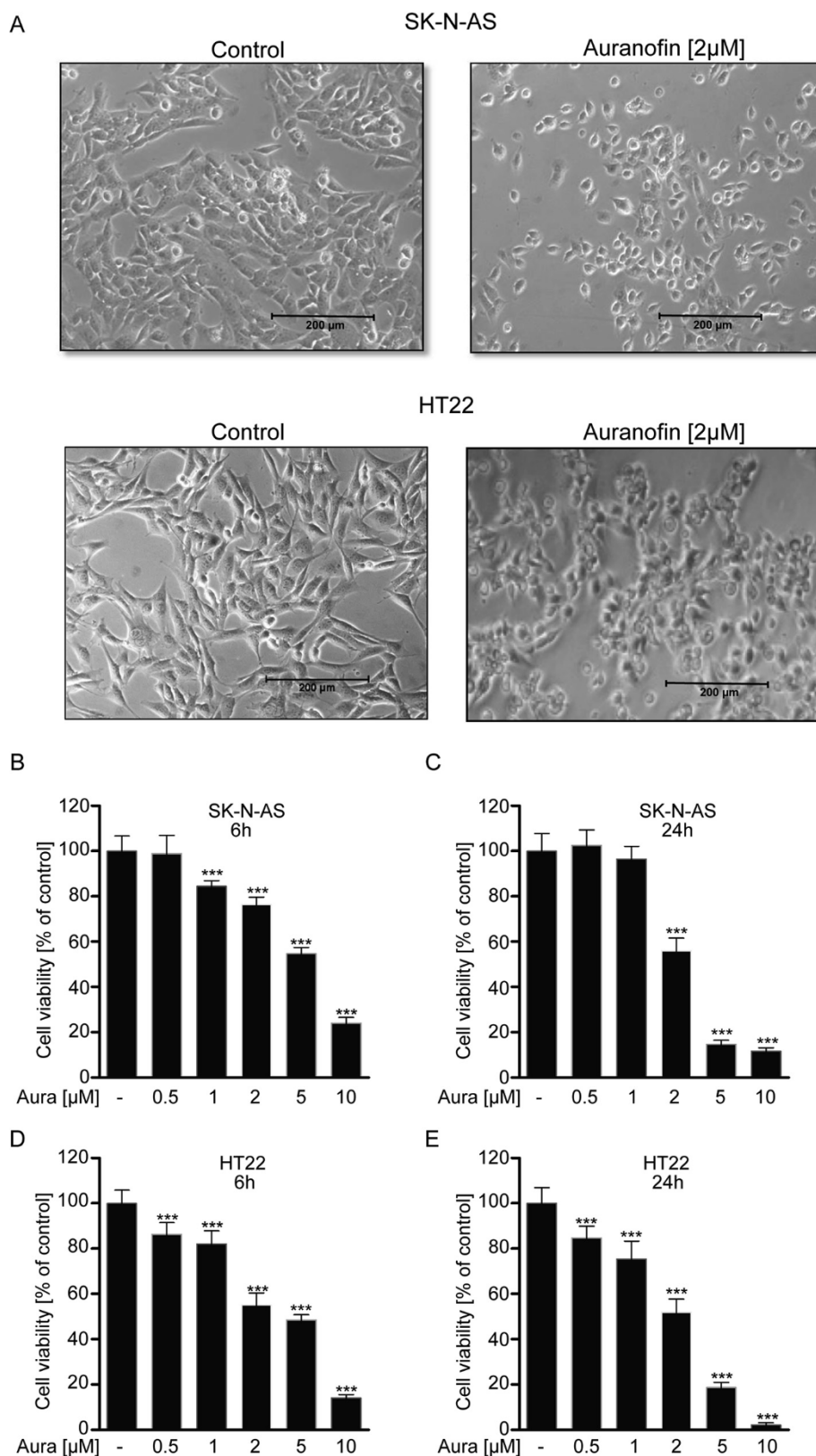
Fig. 1. Auranofin attenuates cell viability in SK-N-AS and HT22 cells. (A) Representative pictures of SK-N-AS and HT22 cells after 6 h auranofin treatment. Scale bar represents 200 μm. (B–E) MTT assay analysis of SK-N-AS and HT22 cells treated with different auranofin (shortened as 'Aura') concentrations (0.5–10 μM, 6 & 24 h, n = 6). Data are presented as mean ± SD; ***$p < 0.001$, *compared to control.

alone, as shown by PI FACS measurements, a method used to complement the crystal violet assay, where the dead cells were eliminated during the procedure. Nevertheless, combined treatment of 2 μM

auranofin with high CyPPA concentrations (50 μM) induced more cell death when compared to auranofin alone or combined with low CyPPA concentrations (10 μM) (Fig. 2F). These data indicate that CyPPA
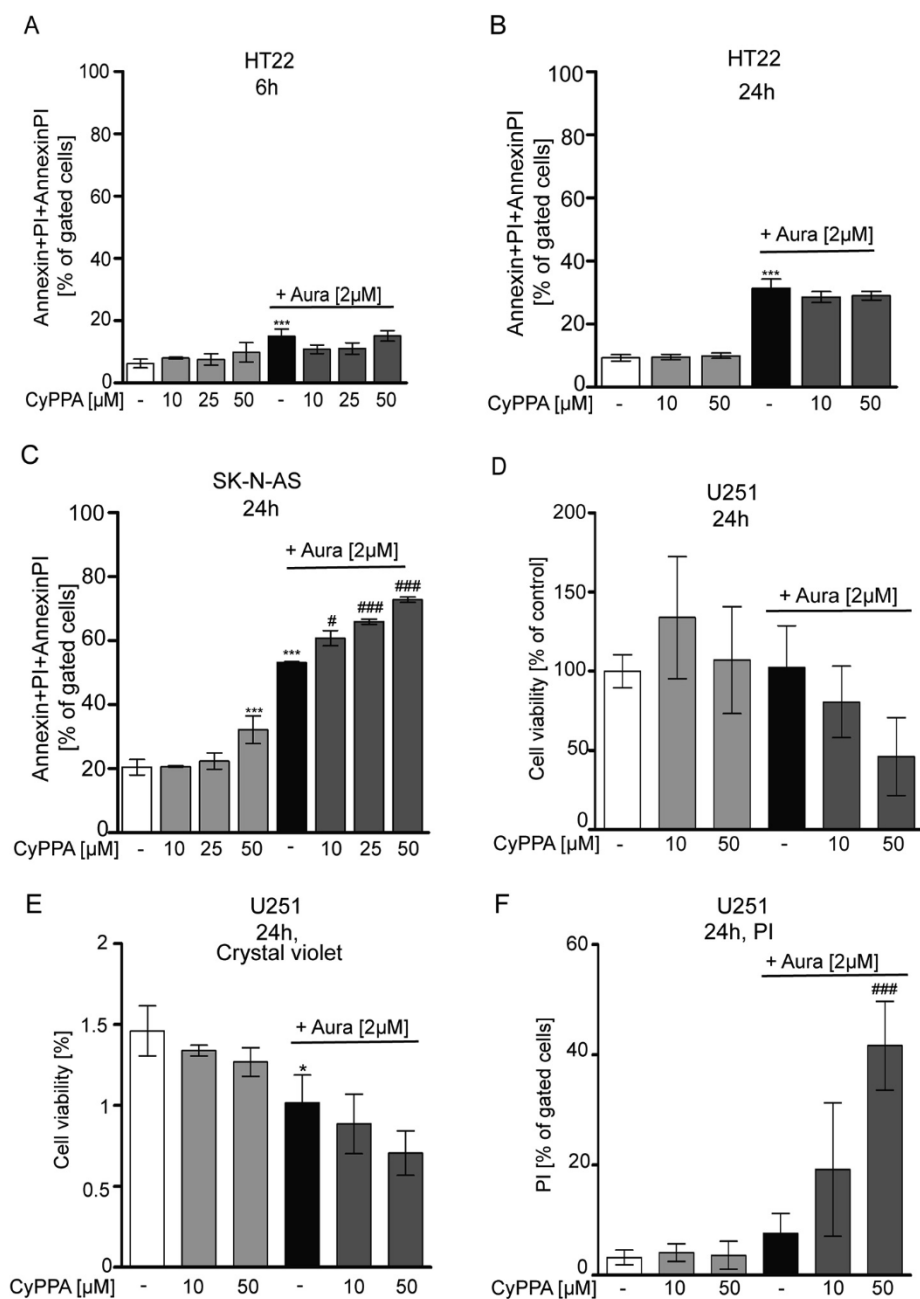
Fig. 2. SK channel activation potentiates auranofin-induced cell death in SK-N-AS and U251 cells. (A–C) AnnexinV/PI fluorescence of SK-N-AS and HT22 cells treated with different CyPPA concentrations (10–50 μM) in the presence or absence of auranofin (2 μM, 6 h (A) or 24 h (B, C), n = 3). (D-F) U251 cells treated with different CyPPA concentrations (10 and 50 μM) in the presence or absence of auranofin (2 μM, 24 h). Cell viability is shown by MTT assay (D), proliferation assay crystal violet (E) and PI fluorescence (F). Data are presented as mean ± SD, n = 6, *$p < 0.05$, ***$p < 0.001$ compared to control, #$p < 0.05$, ##$p < 0.01$, ###$p < 0.001$, compared to auranofin alone.

significantly contributes to auranofin cytotoxicity in human glioblastoma cells.
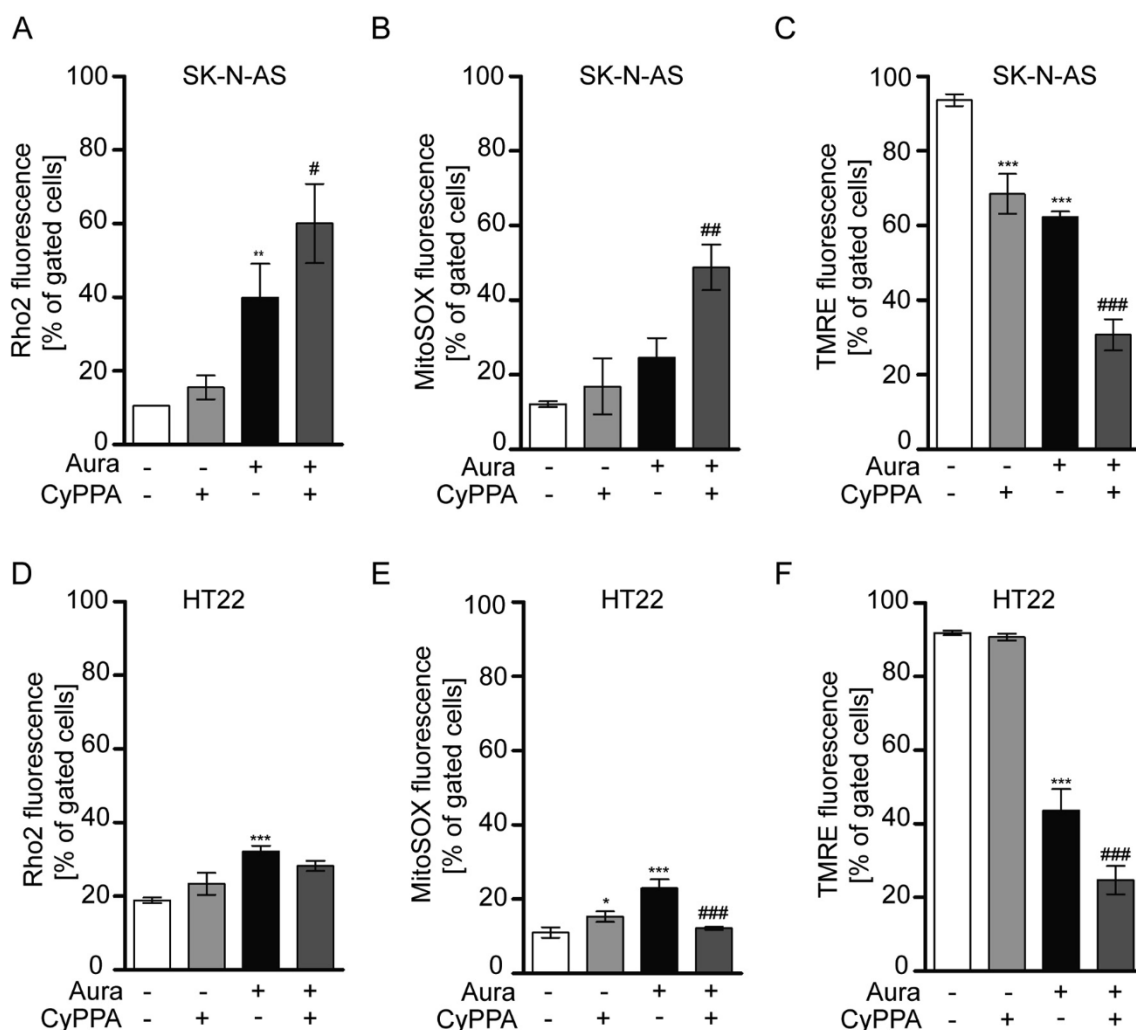
3.2. Combined auranofin and CyPPA treatment promotes mitochondrial damage in SK-N-AS cells

Several studies showed that auranofin mediated depolarisation of the mitochondrial transmembrane potential (MMP), promoted the formation of the mPTP and increased ROS levels [30–32]. Furthermore, previous results from our lab indicated that SK channel activation alone induced a mild increase in mitochondrial ROS and a slight decrease in the MMP [38], suggesting that a combination of CyPPA and auranofin might augment auranofin-induced mitochondrial damage. Therefore, we next investigated the effect of 24 h auranofin (2 μM) in the presence or absence of CyPPA (10 μM) on mitochondrial parameters typically associated with oxidative dysbalance and mitochondrial dysfunction in SK-N-AS cells.

It has been reported that auranofin increases mitochondrial calcium (mito[Ca^{2+}]) levels, thereby promoting mPTP opening [34]. In our study, mito[Ca^{2+}] levels were mildly increased upon auranofin treatment, and there was an additional effect of CyPPA (Fig. 3A). Next, we tested mitochondrial ROS following auranofin treatment and detected that auranofin alone slightly increased mitochondrial ROS levels in SK-N-AS cells, an effect being potentiated by co-treatment of CyPPA (Fig. 3B). We observed a decrease in MMP after auranofin treatment that was even further reduced in combination with CyPPA (Fig. 3C). Furthermore, levels of cytosolic ROS were increased in response to auranofin (Fig. 4A). Cytosolic ROS induced by auranofin was further increased when CyPPA was present (Fig. 4A). Similar to mitochondrial ROS levels, auranofin increased general lipid peroxidation, a phenomenon that was potentiated by CyPPA (Fig. 4B). Pre-treatment with ROS scavenger *N*-acetyl-L-cysteine (NAC) antagonized the cell damage mediated by auranofin in both SK-N-AS cells and HT22 cells (Fig. 4D and G).

In contrast, in HT22 cells, co-treatment with CyPPA prevented accumulation of mito[Ca^{2+}], mitochondrial ROS and lipid peroxidation

Fig. 3. Auranofin and CyPPA combination treatment induces mitochondrial-related dysfunction. SK-N-AS cells and HT22 cells treated with auranofin (2 μM, 24 h or 6 h) in the presence or absence of CyPPA (10 μM or 50 μM, n = 3). (A & D) Mitochondrial calcium (Rho2-AM), (B & E) Mitochondrial superoxide levels (MitoSOX), (C & F) MMP loss (TMRE) were determined by FACS analysis.. Data are presented as mean ± SD, $*p < 0.05$, $**p < 0.01$, $***p < 0.001$, $^{\#}p < 0.05$, $^{\#\#}p < 0.01$, $^{\#\#\#}p < 0.001$, *compared to control $^{\#}$compared to auranofin alone.

(Figs. 3D, E, 4F) compared with auranofin treatment alone, indicating a milder CyPPA effect in neuronal HT22 cells compared to a detrimental effect in neuroblastoma SK-N-AS cells. Cytosolic ROS levels and MMP were similarly affected in both, SK-N-AS and HT22 (Figs. 3F and 4E) cells, i.e., SK channel activation potentiated the auranofin-induced increase in cytosolic ROS and further reduced MMP in the presence of auranofin compared to auranofin treatment alone. Collectively, these results suggest that SK channel activation potentiates auranofin-induced mitochondrial dysfunction in neuroblastoma SK-N-AS cells.

3.3. The auranofin-induced decrease in mitochondrial respiration is enhanced by SK channel activation

So far, we showed that SK-N-AS cells are vulnerable to cell death and mitochondrial dysfunction induced by auranofin which was potentiated by SK channel activation. In contrast, auranofin-mediated cell death was not potentiated by the presence of CyPPA in HT22 cells.

Since SK channel activation decreases mitochondrial respiration, we next studied this feature of CyPPA, together with auranofin, at the functional level of mitochondrial respiration. To investigate this, we treated both cell lines with auranofin with or without CyPPA and measured mitochondrial bioenergetics using the Seahorse extracellular flux technology. Regarding mitochondrial OCR values, in SK-N-AS cells,

there was a dose-dependent reduction in basal respiration following auranofin treatment (Fig. 5A and B). Basal respiration was also reduced in response to auranofin (2 μM) treatment in the presence of CyPPA (10 μM) (Fig. 6). Auranofin alone had minor effects on basal respiration in HT22 cells (Fig. 5D and E), but the addition of CyPPA reduced basal respiration (Fig. 6D and E).

In both cell lines, auranofin reduced the maximal uncoupled respiration, reflecting the maximum activity of the electron transport, in a dose-dependent manner. However, in SK-N-AS cells, the maximal respiration was highly reduced in the presence of auranofin compared to auranofin-exposed HT22 cells (Fig. 5C and F), indicating that the sensitivity of SK-N-AS to auranofin exposure was much higher compared to HT22 cells. While mild effects on maximal respiration were evoked by 2 μM auranofin in HT22 cells, a four-fold lower concentration (0.5 μM) of auranofin massively impaired maximal respiration in SK-N-AS cells. The addition of CyPPA potentiated the reduction in maximal respiration in the presence of auranofin in both SK-N-AS and HT22 cells, however with a stronger effect in neuroblastoma SK-N-AS cells (Fig. 6A and C) compared to neuronal HT22 cells (Fig. 6D and F). ECAR values changed in response to high concentration of auranofin only in SK-N-AS cells and CyPPA application had no additional effects in neither SK-N-AS (Fig. 5G and H) nor HT22 cells (data not shown). Taken together, we showed that CyPPA promoted the auranofin-induced decrease in mitochondrial
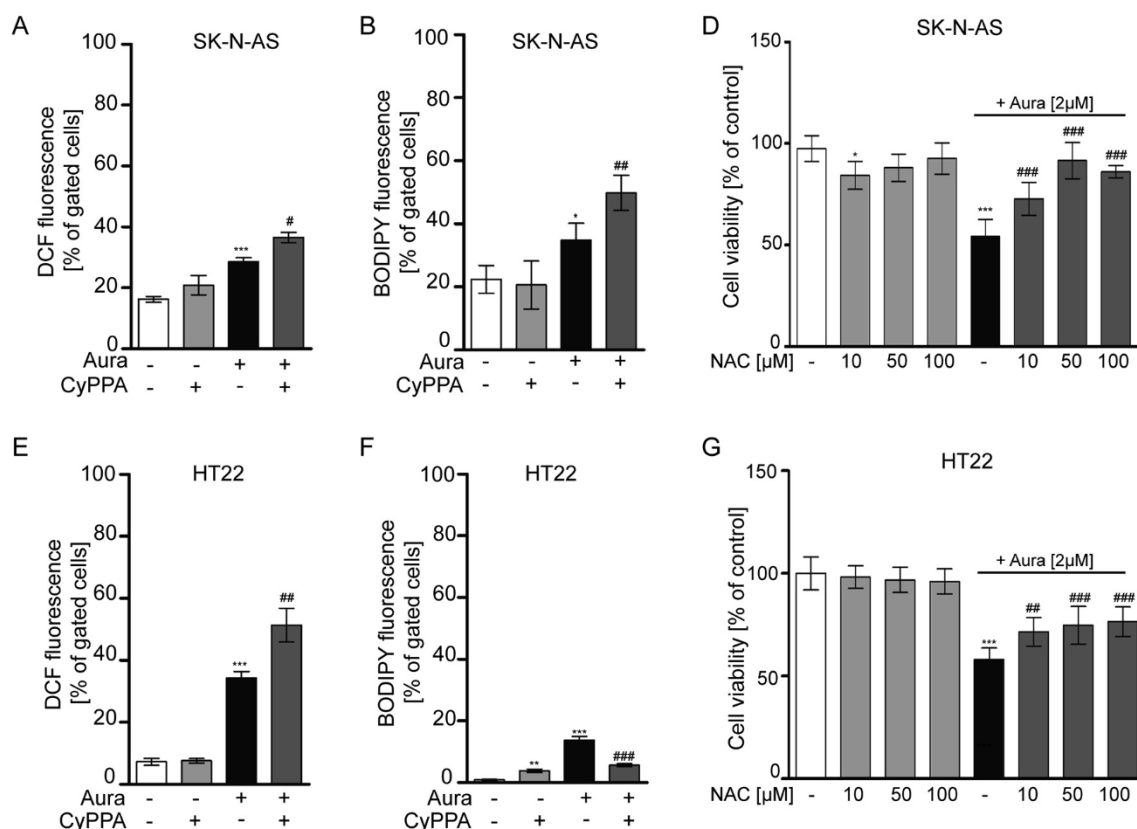
Fig. 4. Combination treatment of auranofin and CyPPA induces oxidative dysbalance. SK-N-AS cells and HT22 cells treated with auranofin (2 μM, 24 h or 6 h) in the presence or absence of CyPPA (10 μM or 50 μM, n = 3) (A & E) cellular ROS (H$_2$DCFDA, depicted as DCF) and (B & F) lipid peroxidation levels (Bodipy) were determined by FACS analysis. (D & G) MTT assay of SK-N-AS and HT22 cells treated with different NAC (10–100 μM) concentrations in the presence or absence of auranofin (2 μM), 24 h. Data are presented as mean ± SD, n = 3–6; *$p < 0.05$, **$p < 0.01$, ***$p < 0.001$, ##$p < 0.01$, ###$p < 0.001$, *compared to control #compared to auranofin alone.

respiration. In line with our findings on mitochondrial damage, SK-N-AS cells were more sensitive to auranofin treatment regarding the mitochondrial metabolism compared with HT22 cells.

3.4. Combined auranofin and CyPPA application reduces cell invasiveness

3D spheroids recapitulate cell–cell and cell-matrix interactions between tumour cells and the microenvironment [39], for what they had become widely used for tumour growth drug screening [40]. In addition, 3D spheroids embedded in a matrix, allow studies of cellular invasion and matrix remodeling [41]. Thus, to verify our findings, a 3D invasion assay was performed using U251 spheres on a collagen matrix, followed by treatment with auranofin and CyPPA. As observed in Fig. 7, auranofin and CyPPA combination treatment for 7 days (168 h) completely inhibited the invasion abilities of U251 spheres, as compared to non-treated controls. Similarly, 10 μM or 50 μM CyPPA treatment alone for 7 days decreased invasiveness of cells. It is important to mention that 2 μM auranofin in the absence or presence of CyPPA treatment at short times (24 h and 48 h) already reduced the invasion (see Fig. 7B). However, at the endpoint of 7 days all the treatments completely decreased the cellular invasiveness compared to control, and there were no statistically significant differences between the treatments (Fig. 7C).

3.5. Patient-derived GBM neurospheres show increased auranofin sensitivity upon SK channel activation

To extend our findings in SK-N-AS and U251 cells to generated patient-derived GBM neurospheres, providing a cancer stem cell-enriched 3D model, we employed GG16 neurospheres. Similar to SK-N-AS cells, GG16 cells expressed both SK2 and SK3 subtype of SK channels

(data not shown), while HT22 cells express only the SK2 subtype [42]. The neurospheres were treated with either auranofin alone or in combination with CyPPA and cell viability was analysed. Auranofin dose-dependently decreased cell viability over 24 h (Fig. 8A). However, no additional effects of CyPPA were observed at this time point (Fig. 8B). Prolonging the treatment to 48 h revealed additional damage by CyPPA in the presence of auranofin (Fig. 8C). However, CyPPA itself did not affect cell viability in neurospheres at 48 h. Morphological analysis of the spheres and Annexin/PI double staining confirmed that auranofin-induced cell death was potentiated by CyPPA co-treatment (Fig. 8D and E). As shown by the images (Fig. 8E), auranofin treatment increased the cell debris and the disintegration of neurosphere structure, which was augmented by the presence of CyPPA. Together with our previous findings on cell death in SK-N-AS and U251 cells, these results indicate that patient-derived GBM neurospheres are sensitive to auranofin-induced cell death that can be potentiated by activation of SK channels.

4. Discussion

Our findings demonstrate that auranofin-induced cell death is potentiated by SK channel activation in different brain cancer models. SK channel activation is well known to confer protection in different models of brain damage *in vitro and in vivo*, including middle cerebral artery occlusion [43,44]. However, little is known about its effect on brain cancer development or progression. Recent studies showed that potassium channels, in particular K$_{Ca}$ channels, can modulate mitochondrial activity [38], and thus might potentiate the effects of anticancer treatments through this mechanism. In this study, we found that SK channel activation was able to increase auranofin-induced toxicity in glio- and neuroblastoma/GBM cell lines, suggesting that targeting SK
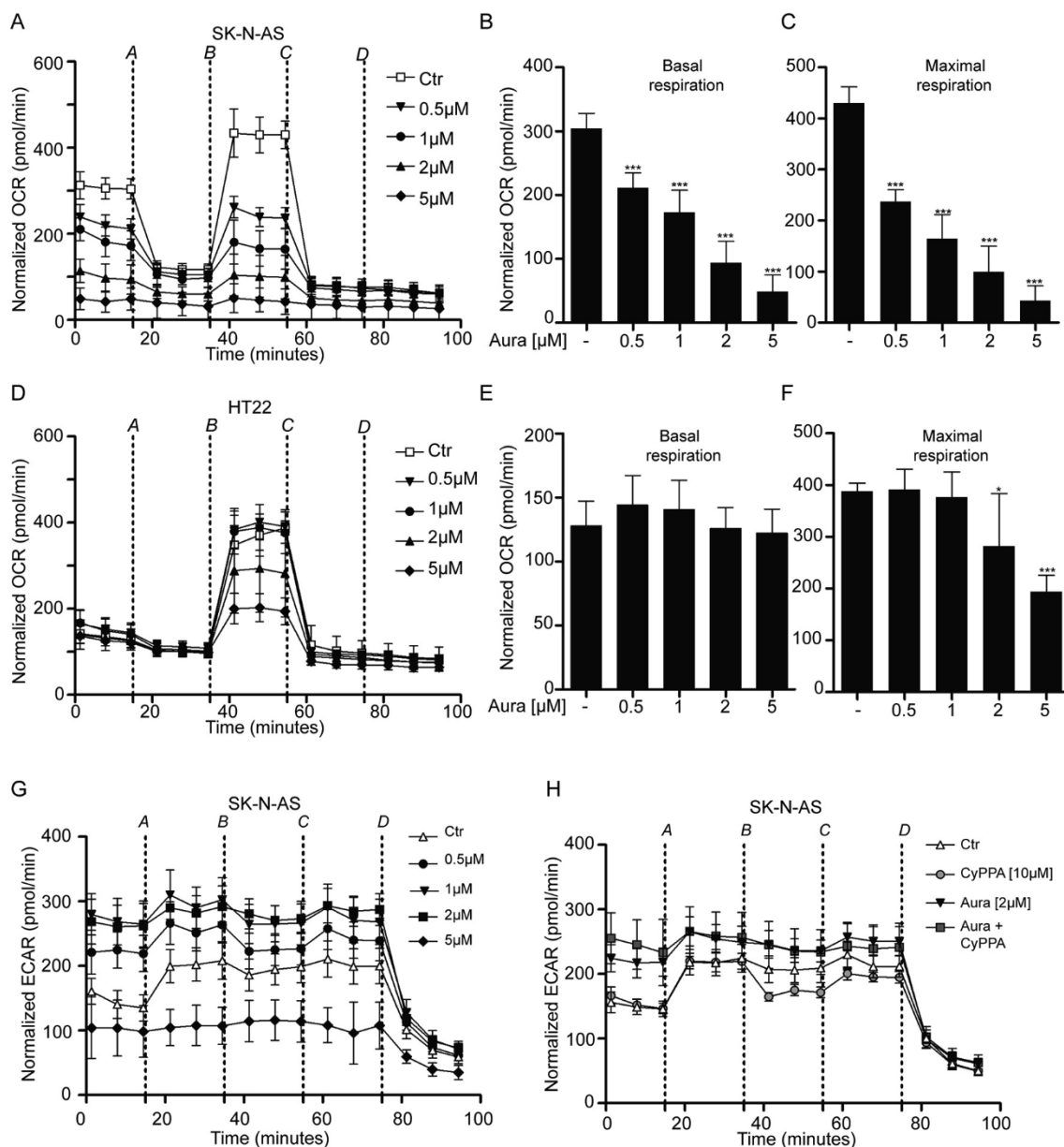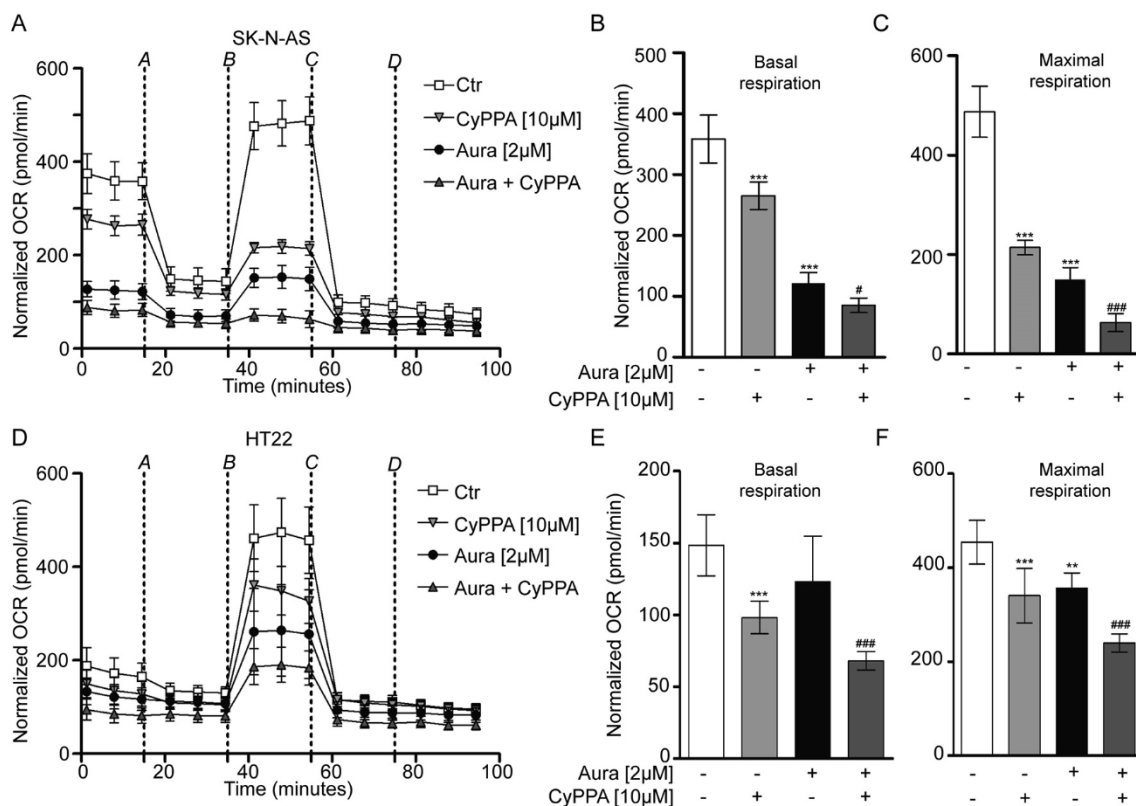
Fig. 5. Auranofin reduces mitochondrial metabolism. (A–F) Representative experiment showing oxygen consumption rate (OCR), basal respiration and maximal respiration in SK-N-AS cells and HT22 cells following treatment with different auranofin concentrations (0.5–5 μM). (G, H) Representative measurement of the extracellular acidification rate (ECAR) in SK-N-AS cells following treatment with different auranofin concentrations (0.5–5 μM) or (G) auranofin (2 μM) with or without CyPPA (10 μM) (H). Injections indicated by the arrow represent (*A*) oligomycin, (*B*) FCCP/DNP, (*C*) rotenone + antimycin A and (*D*) 2-DG. Data are presented as mean ± SD, n = 6 per condition; *$p < 0.05$, **$p < 0.01$, ***$p < 0.001$, #$p < 0.05$, ###$p < 0.001$, *compared to control #compared to auranofin alone.

channels might augment the anti-cancer effects of current treatments.

Recently, it was shown that auranofin decreased the expression of anti-apoptotic protein Bcl-2, and potentiated the expression of pro-apoptotic proteins in cervical cancer HeLa cells and hepatocellular carcinoma Hep3B cells. Treatment with pan-caspase inhibitors significantly prevented the loss of cell viability in both cell lines, suggesting that auranofin induces caspase-dependent apoptosis [45,46]. Inhibition of caspases 8 and 9 was able to attenuate the auranofin-induced cell death in HeLa cells [45]. In addition, auranofin increased the expression of membrane-bound death receptors 4 and 5 in Hep3B cells and the accumulation of truncated Bid [46]. Furthermore, auranofin stimulated the release of lactate dehydrogenase in auranofin-treated HeLa cells [45]. Here, we could confirm that auranofin also induced cell death in different brain cancer cell models, including neuroblastoma SK-N-AS cells, glioblastoma U251 cells, GBM neurospheres and non-

cancerous hippocampal HT22 cells.

Next to Trx, glutathione (GSH) plays an essential role in the cellular detoxification of ROS [47,48]. Activation of SK channels protects against conditions of GSH deficiency, and oxidative toxicity in healthy neurons [42,49]. Interestingly, many studies probed for inhibition of SK channels to induce cytotoxic effects in different types of cancer. It was found that knockdown of SK channels exerted cytotoxic effects in breast cancer cells [16], and inhibition of SK channels by apamin significantly improved performance in mice with neurofibromatosis [50]. Other members of the K_{Ca} channel family were also related to tumour invasion, cell death and immunogenicity [11,51]. Here, we showed that SK channel activation strengthened auranofin-induced toxicity in neuroblastoma, glioblastoma and GBM cells. Although CyPPA alone reduced invasiveness in U251 spheres and showed reduced cell metabolic activity according to the MTT assay in SK-N-AS cells, we found that

Fig. 6. CyPPA potentiates auranofin-induced reduction in mitochondrial metabolism. (A–F) Representative experiment showing oxygen consumption rate (OCR), basal respiration and maximal respiration in SK-N-AS cells and HT22 cells following treatment with auranofin (2 μM) with or without CyPPA (10 μM). Injections indicated by the arrow represent (*A*) oligomycin, (B) FCCP/DNP, (C) rotenone + antimycin A and (D) 2-DG. Data are presented as mean ± SD, n = 6 per condition; *$p < 0.05$, **$p < 0.01$, ***$p < 0.001$, #$p < 0.05$, ###$p < 0.001$, *compared to control #compared to auranofin alone.

CyPPA alone did not affect cell survival. However, the combination with auranofin promoted apoptosis in both SK-N-AS cells and U251 cells. The combination therapy did not change compared to auranofin monotherapy in HT22 cells, indicating no additional effects in non-cancerous cells. These findings prompt us to conclude a benefit of combination versus auranofin monotherapy in brain cancer cells.

Mitochondrial function is essential in the tumour capacity to invade the surrounding tissues and its own survival. To better understand the effects of the combinatorial approach of auranofin and SK channel activation on mitochondrial integrity in SK-N-AS and HT22 cells, we investigated mitochondrial function. Different types of cancer cells are found to be susceptible to changes in intracellular ROS and decreased MMP [52,53]. Auranofin blocks TrxR activity, thereby impairing the generation of antioxidants and increasing the levels of ROS. This increase in ROS levels is associated with formation of mPTP and Ca^{2+}-dependent cell death [34]. In the present study, we observed an increase in mito[Ca^{2+}], loss of MMP, increased lipid peroxidation, mitochondrial- and cytosolic ROS levels in both SK-N-AS and HT22 cells following auranofin treatment. ROS generation is necessary for the auranofin-induced apoptosis in Hep3B cells [46]. However, the capacity of auranofin to induce ROS is different in distinct cancer cell types. While auranofin-induced oxidative stress is limited in THP-1 and Jurkat T cells, ROS levels increased upon auranofin treatment in Hep3B cells and MEC-1 cells [32,33,46,54]. Treatment with the antioxidant NAC attenuated auranofin-induced cell death in HeLa cells, Hep3B cells, MEC-1 and CCLs [32,46] and pre-treatment with NAC also completely prevented auranofin-induced inactivation of TrxR in Hep3B cells. In our study, pre-treatment with NAC partially reduced cell death induced by auranofin in both SK-N-AS cells and HT22 cells, suggesting a role for oxidative stress in auranofin toxicity. SK channel activation potentiated all mitochondrial dysfunction parameters in SK-N-AS cells to toxic

levels following auranofin exposure, indicating that CyPPA as a combination treatment promotes cancer cell death by enhancing mitochondrial damage.

In contrast to SK-N-AS cells, SK channel activation protected HT22 cells from the increase in mitochondrial superoxides, mito[Ca^{2+}] and lipid peroxidation following auranofin exposure. SK channels have often been shown to be protective in different conditions of Ca^{2+} dysregulation and oxidative stress [55–58], and in our previous studies in HT22 cells, CyPPA decreased the uptake of mito[Ca^{2+}] in conditions of oxidative stress [38] and also following increased ER-mitochondria contact sites [58]. The lack of apoptosis induction following auranofin and CyPPA combination treatment in HT22 cells may stem from the observed reduction in toxic ROS and mito[Ca^{2+}]. Therefore, the distinct effect of combinatorial treatment in HT22 cells may reflect in minimal side effects on non-cancerous cells.

Recent evidence suggests that SK channel activation by CyPPA and/or overexpression of mitochondrial SK2 in mammalian cells attenuates mitochondrial respiration [34]. In contrast, inhibition of the respiratory chain by auranofin was only shown in yeast [59], but knowledge on the metabolic effect of auranofin in brain cancer cells was lacking so far. We found that auranofin blocked maximal respiration. Notably, SK-N-AS cells revealed an increased sensitivity towards both, auranofin-mediated and CyPPA-mediated impairment of basal and maximal mitochondrial respiration compared to neuronal HT22 cells. In line, the combination treatment evoked detrimental effects in SK-N-AS, but less in HT22 cells. Especially maximal respiration was highly reduced in SK-N-AS cells compared to HT22 cells. Therefore, the increased sensitivity may contribute to the potentiation effect when auranofin and CyPPA are combined in SK-N-AS cells but not in HT22 cells suggesting a potential cell-type specificity in brain cancer cells.

To extend our data to a broader concept, we evaluated the effects of
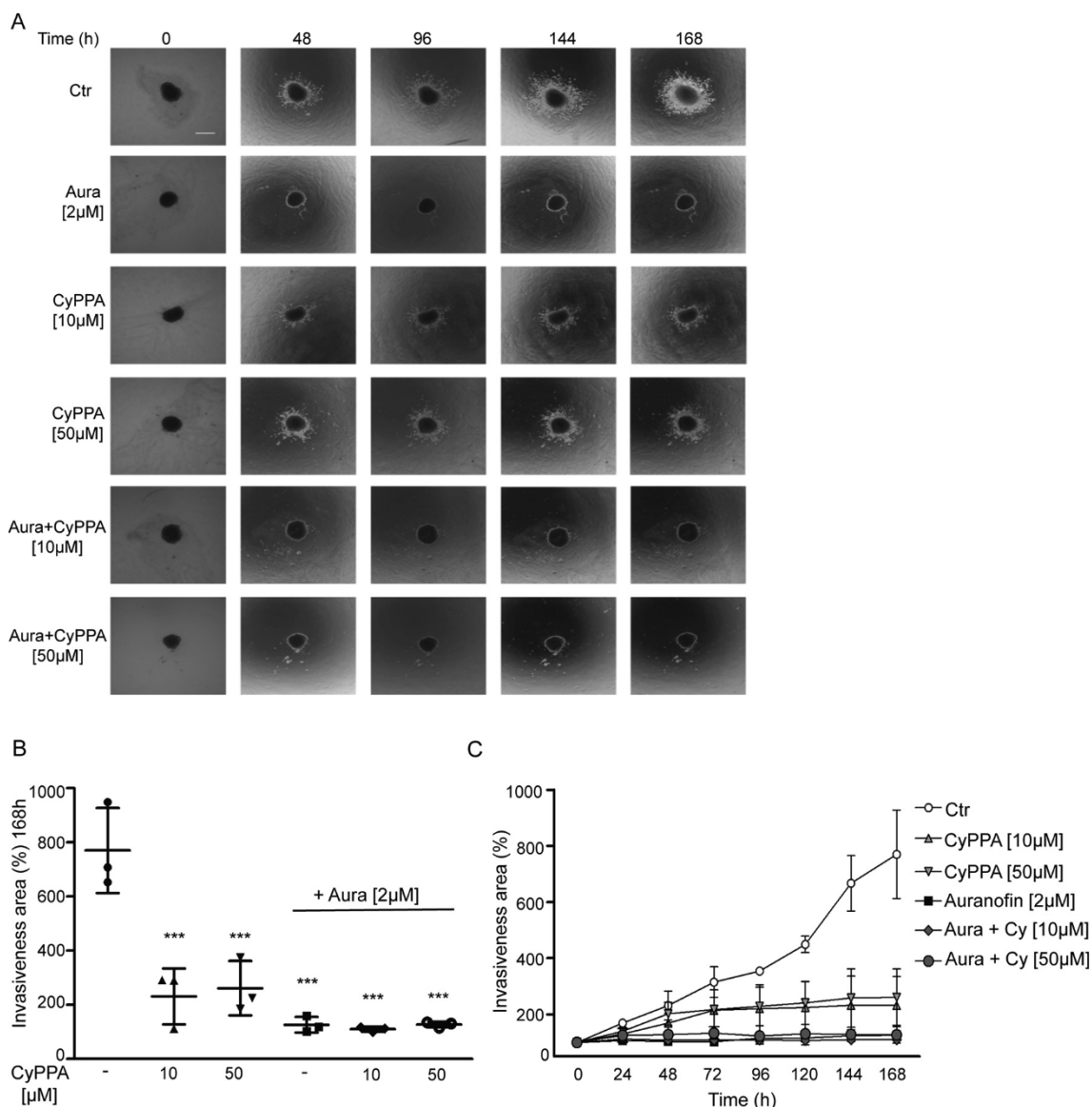
Fig. 7. Auranofin and CyPPA treatment reduce U251 spheroid invasiveness. (A) Bright-field images at 4X magnification from tumor spheroids treated with auranofin in the presence or absence of CyPPA (10 μM or 50 μM) for 7 days/168 h. The invasiveness area of spheroids for 7 days (B) and final day (C) are plotted. Data represents the mean ± SD, n = 3; $^{*}p < 0.05$; $^{**}p < 0.01$; $^{***}p < 0.001$; $^{****}p < 0.0001$; ns, not significant. Scale bar: 0.25 mm.

auranofin and SK channel activation in patient-derived GBM neurospheres. We showed that auranofin was toxic to these neurospheres and that again SK channel activation potentiated auranofin-induced cell death. Increasing evidence indeed indicates a role for ROS-based treatment for GBM tumours specifically, without affecting other cell types in the brain [60,61]. Moreover, auranofin toxicity in GBM tumours has been shown previously [62,63]. However in the present study we show that it is possible to induce even more damage through SK channel activation than with auranofin alone. The combination therapy of auranofin and CyPPA could, therefore, represent a promising approach for the treatment of GBM tumours, however, additional experiments using GBM neurospheres derived from more patients are necessary to be tested. Furthermore, proof-of-concept studies in animal models will provide more insights into this new approach.

In conclusion, we show that SK channel activation potentiated auranofin-induced cell death in neuroblastoma cells, glioblastoma cells, and in GBM neurospheres. We conclude that cell death by auranofin and SK channel activation in cancer cells involves ROS generation and attenuated mitochondrial respiration. Therefore, CyPPA, as an additional component to auranofin monotherapy represents a promising strategy for efficient brain tumour therapy.
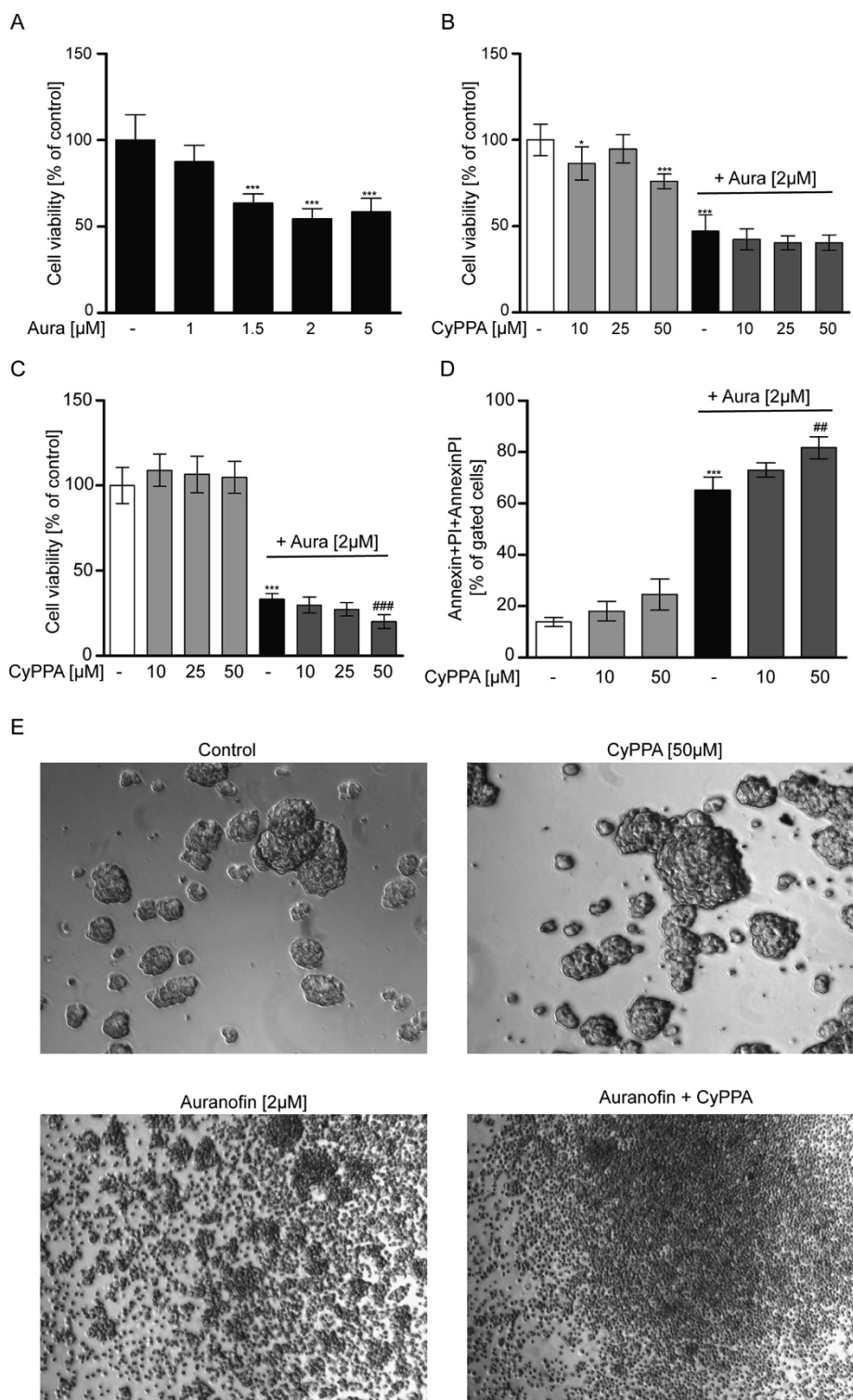
Declaration of Competing Interest

The authors declare that they have no known competing financial interests or personal relationships that could have appeared to influence the work reported in this paper.

Acknowledgements

Fig. 8. SK channel activation enhances auranofin-induced toxicity in patient-derived glioblastoma neurospheres. (A) MTS assay in neurospheres after 24 h auranofin (0–5 μM) treatment and (B) treatment with different CyPPA concentrations in the absence or presence of 2 μM auranofin for 24 h or 48 h (C). (D) AnnexinV/PI fluorescence following treatment with different CyPPA concentrations (10 μM or 50 μM) in the presence or absence of 2 μM auranofin for 48 h. Data are presented as mean ± SD, n = 3–6; $^{***}p < 0.001$ compared to control, $^{##}p < 0.01$, $^{###}p < 0.001$, compared to auranofin alone. (E) representative brightfield images after 48 h treatment with auranofin (2 μM), CyPPA (50 μM) or the combination.

Author contribution

I.E.K. and B.H designed and realized the experiments, analyzed the data and wrote the paper; L.B performed experiments on HT22 and SK-N-AS cells; N.M.P.F. contributed to GBM experiments. E.S-P and H.H performed the experiments on U251 cells and the generation of spheroids for 3D invasion. M.S; F.D. and C.C interpreted data and reviewed the manuscript; J.C.C; F.K and A.M.D. designed, analyzed and interpreted the data, prepared the manuscript and provided critical revision. All authors read and approved the final manuscript.

References

[1] C.U. Louis, J.M. Shohet, Neuroblastoma: molecular pathogenesis and therapy, Annu. Rev. Med. 66 (2015) 49–63, https://doi.org/10.1146/annurev-med-011514-023121.

[2] S.J. Tomolonis, J.A.S. Agarwal, Neuroblastoma pathogenesis: deregulation of embryonic neural crest development, Cell Tissue Res. 372 (2018) 245–262, https://doi.org/10.1002/cncr.27633.Percutaneous.

[3] J.A. Schwartzbaum, J.L. Fisher, K.D. Aldape, M. Wrensch, Epidemiology and molecular pathology of glioma, Nat. Clin. Pract. Neurol. 2 (2006) 494, https://doi.org/10.1038/ncpneuro0289.

[4] J.S. Barnholtz-Sloan, A.E. Sloan, A.G. Schwartz, Relative survival rates and patterns

of diagnosis analyzed by time period for individuals with primary malignant brain tumor, 1973–1997, J. Neurosurg. 99 (2003) 458–466, https://doi.org/10.3171/jns.2003.99.3.0458.

[5] P. Kleihues, D.N. Louis, B.W. Scheithauer, L.B. Rorke, G. Reifenberger, P.C. Burger, W.K. Cavenee, The WHO classification of tumors of the nervous system, J. Neuropathol. Exp. Neurol. 61 (2002) 215–219, https://doi.org/10.1093/jnen/61.3.215.

[6] A. Arcangeli, O. Crociani, E. Lastraioli, A. Masi, S. Pillozzi, A. Becchetti, Targeting ion channels in cancer: a novel frontier in antineoplastic therapy, Curr. Med. Chem. 16 (2009) 66–93, https://doi.org/10.2174/092986709787002835.

[7] L. Jean-Yves, O.-A. Halima, S. Olivier, B. Pierre, A. Ahmed, V. Christophe, Voltage-gated ion channels, new targets in anti-cancer research, Recent Pat. Anticancer. Drug Discov. 2 (2007) 189–202, https://doi.org/10.2174/157489207782497244.

[8] N. Prevarskaya, R. Skryma, Y. Shuba, Ion channels and the hallmarks of cancer, Trends Mol. Med. 16 (2010) 107–121, https://doi.org/10.1016/j.molmed.2010.01.005.

[9] S.P. Fraser, L.A. Pardo, Ion channels: functional expression and therapeutic potential in cancer. Colloquium on Ion Channels and Cancer, EMBO Rep. 9 (2008) 512–515, https://doi.org/10.1038/embor.2008.75.

[10] Amy K. Weaver, Valerie C. Bomben, Harald Sontheimer, Expression and function of calcium-activated potassium channels in human glioma cells AMY, Glia 54 (2009) 223–233, https://doi.org/10.1002/glia.20364.Expression.

[11] N. Hoa, M.P. Myers, T.G. Douglass, J.G. Zhang, C. Delgado, L. Driggers, L.L. Callahan, G. VanDeusen, J.T.H. Pham, N. Bhakta, L. Ge, M.R. Jadus, Molecular mechanisms of paraptosis induction: implications for a non-genetically modified tumor vaccine, PLoS One 4 (2009), https://doi.org/10.1371/journal.pone.0004631.

[12] N.T. Hoa, J.G. Zhang, C.L. Delgado, M.P. Myers, L.L. Callahan, G. Vandeusen, P.M. Schiltz, H.T. Wepsic, M.R. Jadus, Human monocytes kill M-CSF-expressing glioma cells via BK channel activation, (2007) pp. 115–129. doi:10.1038/labinvest.3700506.

[13] Z. Wang, Roles of K+ channels in regulating tumour cell proliferation and apoptosis, Pflugers Arch. Eur. J. Physiol. 448 (2004) 274–286, https://doi.org/10.1007/s00424-004-1258-5.

[14] L.K. Kaczmarek, R.W. Aldrich, K.G. Chandy, S. Grissmer, A.D. Wei, H. Wulff, International Union of Basic and Clinical Pharmacology . C . Nomenclature and Properties of Calcium-Activated and Sodium-Activated Potassium Channels, (2017) 1–11. doi:10.1124/pr.116.012864.

[15] R. Meyer, R. Schönherr, O. Gavrilova-Ruch, W. Wohlrab, S.H. Heinemann, Identification of a ether go-go and calcium-activated potassium channels in human melanoma cells, J. Membr. Biol. 171 (1999) 107–115.

[16] Z.A. Abdulkareem, J.M. Gee, C.D. Cox, K.T. Wann, Knockdown of the small conductance Ca^{2+}-activated K^+ channels is potently cytotoxic in breast cancer cell lines, Br. J. Pharmacol. 173 (2016) 177–190, https://doi.org/10.1111/bph.13357.

[17] T. Finkel, Signal transduction by mitochondrial oxidants, J. Biol. Chem. 287 (2012) 4434–4440, https://doi.org/10.1074/jbc.R111.271999.

[18] Xiaozhuo Chen, Yanrong Qian, Wu Shiyong, The warburg effect: evolving interpretations of an established concept, Free Radic Biol Med. 40 (2015) 1291–1296, https://doi.org/10.1097/CCM.0b013e31823da96d.Hydrogen.

[19] A. Takahashi, N. Ohtani, K. Yamakoshi, S.I. Iida, H. Tahara, K. Nakayama, K.I. Nakayama, T. Ide, H. Saya, E. Hara, Mitogenic signalling and the p16INK4a-Rb pathway cooperate to enforce irreversible cellular senescence, Nat. Cell Biol. 8 (2006) 1291–1297, https://doi.org/10.1038/ncb1491.

[20] M.R. Ramsey, N.E. Sharpless, ROS as a tumour suppressor ? Nat. Cell Biol. 8 (2006) 1213–1215.

[21] C. Sun, H. Zhang, X. Fei Ma, X. Zhou, L. Gan, Y. Yuan Liu, Z. Hua Wang, Isoliquiritigenin enhances radiosensitivity of HepG2 cells via disturbance of redox status, Cell Biochem. Biophys. 65 (2013) 433–444, https://doi.org/10.1007/s12013-012-9447-x.

[22] R.A. Cairns, I. Harris, S. Mccracken, T.W. Mak, Cancer cell metabolism, Cold Spring Harb. Symp. Quant. Biol. 76 (2011) 299–311, https://doi.org/10.1101/sqb.2011.76.012856.

[23] Z. Zou, H. Chang, H. Li, S. Wang, Induction of reactive oxygen species : an emerging approach for cancer therapy, Apoptosis 22 (2017) 1321–1335, https://doi.org/10.1007/s10495-017-1424-9.

[24] M. Hassan, R. Sami, S. Abida, A. Usman, ROS - modulated therapeutic approaches in cancer treatment, J. Cancer Res. Clin. Oncol. 143 (2017) 1789–1809, https://doi.org/10.1007/s00432-017-2464-9.

[25] In Sung Song, Jeong Yu Jeong, Seung Hun Jeong, Hyoung Kyu Kim, Kyung Soo Ko, Byoung Doo Rhee, Nari Kim, Jin Han, Mitochondria as therapeutic targets for cancer stem cells, World J. Stem Cells. 7 418 (2015), https://doi.org/10.4252/wjsc.v7.i2.418.

[26] S. Fulda, L. Galluzzi, G. Kroemer, Targeting mitochondria for cancer therapy, Nat. Rev. Drug Discov. 50 (2018) 124–130, https://doi.org/10.1055/a-0657-4437.

[27] V. Gandin, A. Potamitou, M. Pia, B. Dani, A. Bindoli, F. Sorrentino, F. Tisato, M. Bjo, A. Sturaro, R. Rella, C. Marzano, Cancer cell death induced by phosphine gold(I) compounds targeting thioredoxin reductase, Biochem. Pharmacol. 79 (2010) 90–101, https://doi.org/10.1016/j.bcp.2009.07.023.

[28] G. Powis, W.R. Montfort, Properties and biological activities of thioredoxins, Annu. Rev. Pharmacol. Toxicol. 41 (2001) 261–295.

[29] J. Wang, M. Kobayashi, K. Sakurada, M. Imamura, T. Moriuchi, M. Hosokawa, Possible roles of an adult T-cell leukemia (ATL)-derived factor/thioredoxin in the drug resistance of ATL to Adriamycin, Blood. 89 (1997) 2480–2487.

[30] A. Yokomizo, M. Ono, H. Nanri, Y. Makino, T. Ohga, M. Wada, T. Okamoto, J. Yodoi, M. Kuwano, K. Kohno, Cellular levels of thioredoxin associated with drug sensitivity to cisplatin, mitomycin C, doxorubicin, and etoposide, Cancer Res. 1 (1995) 19.

[31] F. Radenkovic, O. Holland, J.J. Vanderlelie, A.V. Perkins, Selective inhibition of endogenous antioxidants with Auranofin causes mitochondrial oxidative stress which can be countered by selenium supplementation, Biochem. Pharmacol. 146 (2017) 42–52, https://doi.org/10.1016/j.bcp.2017.09.009.

[32] W. Fiskus, N. Saba, M. Shen, M. Ghias, J. Liu, S. Das Gupta, L. Chauhan, R. Rao, S. Gunewardena, K. Schorno, C.P. Austin, K. Maddocks, J. Byrd, A. Melnick, P. Huang, A. Wiestner, K.N. Bhalla, Auranofin induces lethal oxidative and endoplasmic reticulum stress and exerts potent preclinical activity against chronic lymphocytic leukemia, Cancer Res. 74 (2014) 2520–2532, https://doi.org/10.1158/0008-5472.CAN-13-2033.

[33] M.P. Rigobello, A. Folda, B. Dani, R. Menabò, G. Scutari, A. Bindoli, Gold(I) complexes determine apoptosis with limited oxidative stress in Jurkat T cells, Eur. J. Pharmacol. 582 (2008) 26–34, https://doi.org/10.1016/j.ejphar.2007.12.026.

[34] M.P. Rigobello, G. Scutari, R. Boscolo, A. Bindoli, Á. Padova, V.G. Colombo, C. Studio, C. Biologica, B. Cnr, C. Biologica, V.G. Colombo, Induction of mitochondrial permeability transition by auranofin, a Gold(I)phosphine derivative, Br. J. Pharmacol. 136 (2002) 1162–1168.

[35] J.V. Joseph, S. Conroy, T. Tomar, E. Eggens-Meijer, K. Bhat, S. Copray, A.M.E. Walenkamp, E. Boddeke, V. Balasubramanyian, M. Wagemakers, W.F.A. Den Dunnen, F.A.E. Kruyt, TGF-β is an inducer of ZEB1-dependent mesenchymal transdifferentiation in glioblastoma that is associated with tumor invasion, Cell Death Dis. 5 (2014) e1443–e1514, https://doi.org/10.1038/cddis.2014.395.

[36] J.M. Ruijter, C. Ramakers, W.M.H. Hoogaars, Y. Karlen, O. Bakker, M.J.B. van den hoff, A.F.M. Moorman, Amplification efficiency: Linking baseline and bias in the analysis of quantitative PCR data, Nucleic Acids Res. 37 (2009), https://doi.org/10.1093/nar/gkp045.

[37] M.P. Rigobello, G. Scutari, R. Boscolo, A. Bindoli, Induction of mitochondrial permeability transition by auranofinn, a Gold(I)-phosphine derivative, Br. J. Pharmacol. 136 (2002) 1162–1168, https://doi.org/10.1038/sj.bjp.0704823.

[38] B. Honrath, L. Matschke, T. Meyer, L. Magerhans, F. Perocchi, G.K. Ganjam, H. Zischka, C. Krasel, A. Gerding, B.M. Bakker, M. Bünemann, S. Strack, N. Decher, C. Culmsee, A.M. Dolga, SK2 channels regulate mitochondrial respiration and mitochondrial Ca^{2+} uptake, Cell Death Differ. 24 (2017) 761–773, https://doi.org/10.1038/cdd.2017.2.

[39] E. Fennema, N. Rivron, J. Rouwkema, C. van Blitterswijk, J. De Boer, Spheroid culture as a tool for creating 3D complex tissues, Trends Biotechnol. 31 (2013) 108–115, https://doi.org/10.1016/j.tibtech.2012.12.003.

[40] L.B. Weiswald, D. Bellet, V. Dangles-Marie, Spherical cancer models in tumor biology, Neoplasia (United States) 17 (2015) 1–15, https://doi.org/10.1016/j.neo.2014.12.004.

[41] M.E. Katt, A.L. Placone, A.D. Wong, Z.S. Xu, P.C. Searson, In vitro tumor models: Advantages, disadvantages, variables, and selecting the right platform, Front. Bioeng. Biotechnol. 4 (2016), https://doi.org/10.3389/fbioe.2016.00012.

[42] A.M. Dolga, M.F. Netter, F. Perocchi, N. Doti, L. Meissner, S. Tobaben, J. Grohm, H. Zischka, N. Plesnila, N. Decher, C. Culmsee, Mitochondrial small conductance SK2 channels prevent glutamate-induced oxytosis and mitochondrial dysfunction, J. Biol. Chem. 288 (2013) 10792–10804, https://doi.org/10.1074/jbc.M113.453522.

[43] A.M. Dolga, N. Terpolilli, F. Kepura, I.M. Nijholt, H. Knaus, B. D'Orsi, J.H.M. Prehn, U.L.M. Eisel, T. Plant, N. Plesnila, C. Culmsee, KCa2 channels activation prevents [Ca2 +]i deregulation and reduces neuronal death following glutamate toxicity and cerebral ischemia, Cell Death Dis. 2 (2011) e147, , https://doi.org/10.1038/cddis.2011.30.

[44] J. Zhu, L.-K. Yang, W.-L. Chen, W. Lin, Y.-H. Wang, T. Chen, Activation of SK/KCa channel attenuates spinal cord ischemia-reperfusion injury via anti-oxidative activity and inhibition of mitochondrial dysfunction in rabbits, Front. Pharmacol. 10 (2019) 1–12, https://doi.org/10.3389/fphar.2019.00325.

[45] B.R. You, H.R. Shin, B.R. Han, S.H. Kim, W.H. Park, Auranofin induces apoptosis and necrosis in HeLa cells via oxidative stress and glutathione depletion, Mol. Med. Rep. 11 (2015) 1428–1434, https://doi.org/10.3892/mmr.2014.2830.

[46] H. Hwang-Bo, J.-W. Jeong, M.H. Han, C. Park, S.-H. Hong, G.-Y. Kim, S.-K. Moon, J. Cheong, W.-J. Kim, Y.H. Yoo, Y.H. Choi, Auranofin, an inhibitor of thioredoxin reductase, induces apoptosis in hepatocellular carcinoma Hep3B cells by generation of reactive oxygen species, Gen. Physiol. Biophys. 36 (2017) 117–128.

[47] A. Holmgren, C. Johansson, C. Berndt, M.E. Lönn, C. Hudemann, C.H. Lillig, Thiol redox control via thioredoxin and glutaredoxin systems, Biochem. Soc. Trans. 33 (2005) 1375–1377.

[48] T.H. Murphy, M. Miyamoto, A. Sastre, R.L. Schnaar, J.T. Coyle, Glutamate toxicity in a neuronal cell line involves inhibition of cystein transport leading to oxidative stress, Neuron 2 (1989) 1547–1558.

[49] B. Honrath, L. Matschke, T. Meyer, L. Magerhans, F. Perocchi, G.K. Ganjam, H. Zischka, C. Krasel, A. Gerding, B.M. Bakker, M. Bünemann, S. Strack, N. Decher, C. Culmsee, A.M. Dolga, SK2 channels regulate mitochondrial respiration and mitochondrial Ca2+ uptake, Cell Death Differ. (2017) 1–13, https://doi.org/10.1038/cdd.2017.2.

[50] A.J. Kallarackal, J.M. Simard, A.M. Bailey, The effect of apamin, a small conductance calcium activated potassium (SK) channel blocker, on a mouse model of neurofibromatosis 1, Behav. Brain Res. 237 (2013) 71–75, https://doi.org/10.1016/j.bbr.2012.09.009.

[51] K. Steinestel, S. Eder, K. Ehinger, J. Schneider, F. Genze, E. Winkler, E. Wardelmann, A.J. Schrader, J. Steinestel, The small conductance calcium-activated potassium channel 3 (SK3) is a molecular target for Edelfosine to reduce the invasive potential of urothelial carcinoma cells, Tumor Biol. 37 (2016) 6275–6283, https://doi.org/10.1007/s13277-015-4509-5.

[52] G. Lian, F. Li, Y. Yin, L. Chen, J. Yang, Herbal extract of Artemisia vulgaris (mugwort) induces antitumor effects in HCT-15 human colon cancer cells via autophagy

induction, cell migration suppression and loss of mitochondrial membrane potential, J. Buon. 23 (2018) 73–78.

[53] D. Sun, L. Wang, P. Zhang, Y.Y. Hospital, ANTITUMOR EFFECTS OF CHRYSANTHEMIN IN PC-3 HUMAN PROSTATE CANCER CELLS ARE MEDIATED VIA APOPTOSIS INDUCTION, CASPASE SIGNALLING PATHWAY AND LOSS OF MITOCHONDRIAL MEMBRANE POTENTIAL. Department of Urology Surgery, Yantai Yuhuangding Hospital, Yantai, 14 (2017) 54–61.

[54] Y. Omata, J.B. Lewis, P.E. Lockwood, W.Y. Tseng, R.L. Messer, S. Bouillaguet, J.C. Wataha, Gold-induced reactive oxygen species (ROS) do not mediate suppression of monocytic mitochondrial or secretory function, Toxicol. Vitr. 20 (2006) 625–633, https://doi.org/10.1016/j.tiv.2005.11.001.

[55] P. Christophersen, H. Zischka, N. Plesnila, A. Dolga, A. de Andrade, L. Meissner, H.-G. Knaus, M. Höllerhage, P. Christophersen, H. Zischka, N. Plesnila, G.U. Höglinger, C. Culmsee, Subcellular expression and neuroprotective effects of SK channels in human dopaminergic neurons, Cell Death Dis 5 (2014) e999, https://doi.org/10.1038/cddis.2013.530.

[56] M. Richter, N. Vidovic, B. Honrath, P. Mahavadi, R. Dodel, A.M. Dolga, C. Culmsee, Activation of SK2 channels preserves ER Ca2 + homeostasis and protects against ER stress-induced cell death, 23 (2016) 814–827. doi:10.1038/cdd.2015.146.

[57] M. Richter, C. Nickel, L. Apel, A. Kaas, R. Dodel, C. Culmsee, A.M. Dolga, SK channel activation modulates mitochondrial respiration and attenuates neuronal HT-22 cell damage induced by H2O2, Neurochem. Int. 81 (2015) 63–75, https://doi.org/10.1016/j.neuint.2014.12.007.

[58] B. Honrath, I.E. Krabbendam, C. Ijsebaart, V. Pegoretti, N. Bendridi, J. Rieusset,

M. Schmidt, C. Culmsee, A.M. Dolga, SK channel activation is neuroprotective in conditions of enhanced ER – mitochondrial coupling, Cell Death Dis. (2018) 1–11, https://doi.org/10.1038/s41419-018-0590-1.

[59] T. Gamberi, T. Fiaschi, A. Modesti, L. Massai, L. Messori, M. Balzi, F. Magherini, Evidence that the antiproliferative effects of auranofin in Saccharomyces cerevisiae arise from inhibition of mitochondrial respiration, Int. J. Biochem. Cell Biol. 65 (2015) 61–71, https://doi.org/10.1016/j.biocel.2015.05.016.

[60] L. Lv, L. Zheng, D. Dong, L. Xu, L. Yin, Y. Xu, Y. Qi, X. Han, J. Peng, Dioscin, a natural steroid saponin, induces apoptosis and DNA damage through reactive oxygen species : A potential new drug for treatment of glioblastoma multiforme, Food Chem. Toxicol. 59 (2013) 657–669, https://doi.org/10.1016/j.fct.2013.07.012.

[61] J. Mei, F. Pan, L. Li, Q. Rong, Y. Chen, X. Xin, K. Cheng, S. Bin, Z. Shi, A.C. Yu, X. Qian, Piperlongumine selectively kills glioblastoma multiforme cells via reactive oxygen species accumulation dependent JNK and p38 activation, Biochem. Biophys. Res. Commun. 437 (2013) 87–93, https://doi.org/10.1016/j.bbrc.2013.06.042.

[62] R.E. Kast, Glioblastoma invasion, cathepsin B, and the potential for both to be inhibited by auranofin, an old anti-rheumatoid arthritis drug, Zentralbl. Neurochir. 71 (2010) 139–142, https://doi.org/10.1055/s-0029-1242756.

[63] R.E. Kast, G. Karpel-Massler, M.-E. Halatsch, CUSP9* treatment protocol for recurrent glioblastoma: aprepitant, artesunate, auranofin, captopril, celecoxib, disulfiram, itraconazole, ritonavir, sertraline augmenting continuous low dose temozolomide, Oncotarget. 5 (2014) 8052–8082, https://doi.org/10.18632/oncotarget.2408.